ChemComm

COMMUNICATION

View Article Online
View Journal | View Issue

Cite this: *Chem. Commun.*, 2021, 57, 4444

Received 14th January 2021,
Accepted 26th March 2021

DOI: 10.1039/d1cc00244a

rsc.li/chemcomm

A two fluorescent signal indicator-based ratio fluorometric alkaline phosphatase assay based on one signal precursor†

Rongji Wang,[a] Zhihua Wang,*[a] Honghong Rao,[b] Xin Xue,[a] Mingyue Luo,[a] Zhonghua Xue*[a] and Xiaoquan Lu[a]

Two fluorescent signal indicators were simply converted from one organic precursor system by using the superior oxidation capability of manganese dioxide (MnO_2) nanosheets for the first time, finally resulting in the successful fabrication of a ratio fluorometric bioassay of alkaline phosphatase (ALP).

Alkaline phosphatase (ALP), one of the most important phosphate hydrolases in the human body, plays an important role in many physiological reaction processes.[1] The concentration of ALP in normal adults ranges from 40 U L^{-1} to 150 U L^{-1}, and its abnormal level is closely related to many diseases such as hepatobiliary diseases,[2] skeletal system diseases, and tumors.[3] Therefore, the development of a highly sensitive, selective, and reliable method to monitor ALP activity is of great significance for biological systems.[4]

To date, many efforts have been made towards the quantitative analysis of ALP, such as colorimetry,[5,6] electrochemistry,[7,8] fluorometric[9,10] and so on.[11,12] Among these strategies, fluorometric strategies have been widely used due to their extremely high sensitivity and excellent real-time detection performance. Though fluorometric sensors have demonstrated more advantages in various sensing events, most of them usually operate based on the single output readout of fluorescent indicators, such as "turn-off" or "turn-on" mode.[13–16] It, therefore, often results in the limitation of poor spatial resolution and uncomprehensive information for accurate analysis, because of the influences of some unavoidable factors such as the background signal, fluorescent substance concentration, surrounding environment and so on. To solve these drawbacks, a ratiometric fluorescence strategy (ratio-fluorescent sensor) armed with two fluorescent signal indicators was proposed in the past decade and has been widely reported in great successes to obtain more accurate results in various sensing applications.[17–19] Typically, in a ratio fluorometric sensor, target analytes can be designed to sensitively and selectively induce the signal change of two fluorescent signal indicators by presenting two independent fluorescence emission peaks. More significantly, this analyte-dependent asynchronous change of two fluorescent signal indicators is in close correlation to the target content.[20] To this end, the significant signal amplification for analyte analysis can be well demonstrated by integrating the specific two fluorescent signals of "turn-on" and "turn-off" mode. For ALP determination, Xian *et al.* developed a ratiometric fluorescent bioassay by using Ag_2S and calcein as the two fluorescent signal indicators.[21] However, this sensing strategy requires the necessary synthesis of complex fluorescent probes and the sensing principle is mainly due to the incubation interaction between the added fluorescent probes and the target, which limits its further application. Therefore, it is still a challenge to develop a simpler ratio-fluorescence method for detecting ALP.

More recently, manganese dioxide (MnO_2) nanosheets as two-dimensional inorganic nanomaterials have exhibited more potential in MnO_2-based sensing applications, mainly due to their superior light absorption capability, large specific surface area, and easy to form hybrid-based nanoprobes.[22] Unfortunately, most previously developed MnO_2-based fluorescence methods for ALP detection are almost used for single-mode detection, and therefore usually result in poor spatial resolution.[23] Only very few methods related to ratiometric fluorescent sensing performance toward ALP have been explored.[24] So in this study, we attempt to develop a ratio fluorometric ALP biosensor based on a simple system with MnO_2 nanosheets and *o*-phenylenediamine (OPD). As illustrated in Scheme 1, the colorless OPD substrate could easily be catalyzed by MnO_2 nanosheets to form a yellow oxidized product of 2,3-diaminophenazine (oxOPD), a typical fluorescent indicator

[a] *Key Laboratory of Bioelectrochemistry & Environmental Analysis of Gansu Province, College of Chemistry & Chemical Engineering, Northwest Normal University, Lanzhou, 730070, China. E-mail: wangzh@nwnu.edu.cn, xzh@nwnu.edu.cn*

[b] *School of Chemistry & Chemical Engineering, Lanzhou City University, Lanzhou, 730070, China*

† Electronic supplementary information (ESI) available. See DOI: 10.1039/d1cc00244a

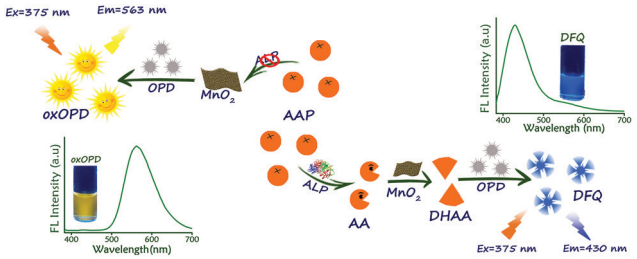

Scheme 1 Schematic illustration of the signal generation process of the ratio fluorometric bioassay for ALP detection.

with a strong yellow fluorescence at 563 nm. This indicator exhibits a sensitive response toward ALP content in the proposed system. With the introduction of ALP, L-ascorbic acid 2-phosphate trisodium salt (AAP) substrate could be hydrolyzed to produce ascorbic acid (AA), and the product AA could be further oxidized by MnO_2 nanosheets to produce dehydroascorbic acid (DHAA). Subsequently, the generated DHAA could rapidly react with OPD to form 3-(1,2-dihydroxy ethyl) furo[3,4-*b*]quinoxalin-1(3*H*)-on (DFQ), a sensitive fluorescent probe with a strong blue fluorescence at 430 nm. As a result, a ratiometric fluorescence sensing platform comprising dual-emission peaks of oxOPD at 563 nm (yellow fluorescence) and DFQ at 430 nm (blue fluorescence) was successfully developed for visual identification of ALP. A small variation in the ratio of the two different fluorescence intensities can lead to an obvious change in the fluorometer color, which can be easily observed with the naked eye and accurately measured with a fluorometer. More importantly, because of the high catalytic activity of MnO_2 nanosheets, the generation of both fluorescent signals in this work is more direct and easy by only using an OPD chromogenic substrate, a special readout generation mode that converts from one signal precursor to two fluorescent signal indicators.

The obtained MnO_2 nanosheets were confirmed by using TEM, FT-IR, XPS, and UV-vis, respectively. As shown in Fig. 1A, MnO_2 samples are two-dimensional nanosheet structures with the typical folds, which is extremely consistent with the previous reports.[23,25] Whereas the confirmation of Mn and O elements in the MnO_2 nanosheets was achieved by using the energy-dispersive X-ray spectroscopy (EDX) spectrum (Fig. 1B), and the FT-IR results (Fig. S1A, ESI†) also confirm the successful formation of the Mn–O bond. Furthermore, the UV-vis absorption spectrum (Fig. 1C) displays a peak at 380 nm of MnO_2 nanosheets.[26] Furthermore, XPS analyses were performed to verify the preparation of MnO_2 nanosheets.[27] A wide scan XPS spectrum shown in Fig. S1B (ESI†) clearly indicates the binding energy peaks of Mn 2p, O 1s, N 1s, and C 1s at 641.6, 528.6, 401.6, and 284.6 eV, respectively. Two characteristic peaks located at 641.2 and 652.95 eV could be attributed to Mn $2p_{3/2}$ and Mn $2p_{1/2}$ (Fig. 1D). All of the above observations indicate the successful preparation of MnO_2 nanosheets.

To further evaluate the feasibility of this ratio fluorometric bioassay for ALP detection, we investigated the fluorescence characteristics of the proposed two fluorescent signal indicator-based system. As shown in Fig. 2A, in the presence of MnO_2 nanosheets, OPD can easily be oxidized to produce oxOPD with a strong yellow fluorescence emission peak at 563 nm. On the other hand, it is well known that AA has two isomers: enol-form and keto-form.[28,29] We found in this system that AA could be oxidized to DHAA in the presence of the appropriate oxidant of MnO_2 nanosheets, and with the presence of OPD, the product DHAA could further react with OPD through a condensation process to form an N-heterocyclic compound with the large conjugated π-bond system, named DFQ, which can emit a strong blue fluorescence at 430 nm (Fig. 2B).[30] However, as displayed in Fig. S2 (ESI†), no fluorescent substance was observed for the reaction system of AA and OPD in the absence of MnO_2 nanosheets. The UV-vis spectrum shown

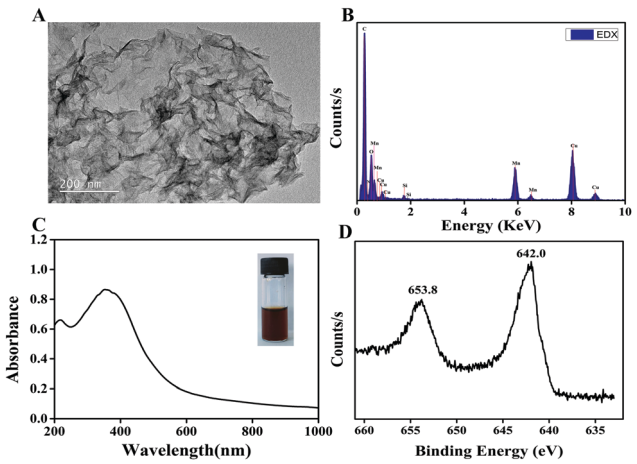

Fig. 1 Characterization of the as-synthesized MnO_2 nanosheet samples. (A) TEM image, (B) EDS spectrum, (C) UV-vis absorbance spectra and the photo of the solution (inset), and (D) XPS spectra of Mn $2p_{3/2}$ and Mn $2p_{1/2}$.

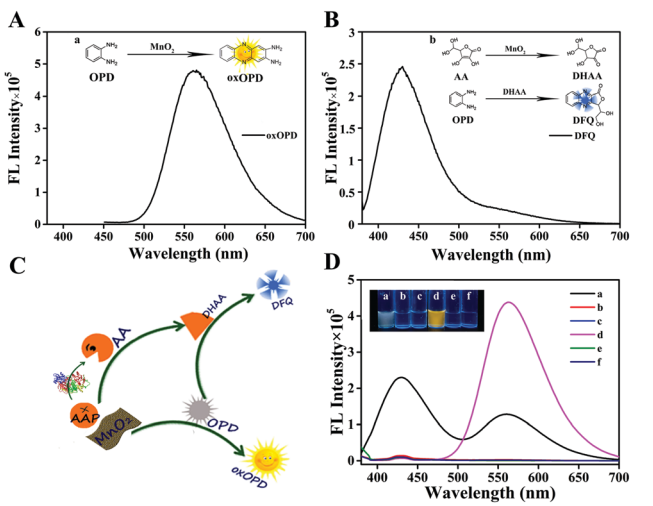

Fig. 2 Schematic illustration of the fluorescent signal generation. (A) oxOPD from the fluorogenic reaction between OPD and MnO_2 nanosheets, (B) DFQ from the fluorogenic reaction of AA + MnO_2 + OPD systems. (C) Schematic diagram of ALP induced two fluorescent signal indicator. (D) Fluorescence emission spectra of (a) AAP+ ALP + MnO_2 + OPD; (b) AAP + MnO_2 + ALP; (c) AAP + MnO_2; (d) ALP + MnO_2 + OPD; (e) AAP + OPD; (f) ALP + OPD in the Tris-HCl buffer solution (20 mM pH = 7.4).

in Fig. S3 (ESI†) also supports the above speculative process. Additionally, we further verified the above reaction features by using a mass spectrometric approach. As displayed in Fig. S4 (ESI†), it is clear that the reaction system of AA and OPD only demonstrated a characteristic mass spectrum peak at 109.07 of OPD and 175.02 of AA, whereas no corresponding mass spectral response of oxOPD, DHAA and DFQ was observed. However, these reaction products and intermediate substances were significantly demonstrated in the presence of MnO_2 nanosheets as shown in Fig. S5 and S6 (ESI†). This may be attributed to the unique feature of this proposed reaction system, in which AA may be oxidized by MnO_2 nanosheets more easily than OPD as supported by some validation experimental results based on zeta potential and electrochemical measurements shown in Fig. S7 (ESI†). Inspired by the previous reports that ALP could exclusively produce AA by hydrolyzing its substrate AAP,[31,32] we believe that ALP could also indirectly trigger the construction of the two fluorescent signal indicator-based fluorescent systems, in which oxOPD and DFQ provide the sensitive fluorescent response. As illustrated in Fig. 2C, firstly, ALP can hydrolyze its substrate AAP to produce AA, and then the redox reaction between AA and MnO_2 nanosheets will happen and produce DHAA. Subsequently, the generated DHAA will react with OPD through a specific condensation process to produce DFQ along with a strong emission peak at 430 nm. Meanwhile, the reduction of both MnO_2 nanosheets and OPD leads to a decrease in the intensity of the emission peak of oxOPD at 563 nm. Thus, a ratio fluorescent platform could be fabricated and used for ALP detection based on the readout change of the fluorescence intensity ratio (F_{563}/F_{430}). To verify the above mechanism, the fluorescent properties of the mixed solvent system containing MnO_2 nanosheets, OPD and AAP were evaluated. As shown in Fig. 2D, with the addition of ALP, both the fluorescence emission peaks corresponding to the oxOPD at 563 nm and the DFQ at 430 nm were clearly observed at the excitation wavelength of 375 nm (Fig. 2D, a), indicating that ALP can successfully trigger the formation of the two fluorescent signal indicator based fluorescent system. Because for the reaction system without ALP introduction, only one fluorescence emission peak corresponding to the oxOPD at 563 nm (Fig. 2D, d) was observed, the fluorescence intensity of oxOPD was significantly higher than that of the ALP added reaction system. In particular, for the reaction system of AAP, ALP and OPD without MnO_2 nanosheets, no obvious fluorescence response could be observed (Fig. S8, ESI†). All these observations suggest a successful construction of this proposed fluorometric system with an ALP-dependent two fluorescent signal response, indicating a potential application of this platform for sensitively sensing ALP.

The fluorometric performance of these developed two fluorescent signal indicators was also estimated at varied excitation light sources (355, 365, 375, 385 nm). As shown in Fig. S9 (ESI†), the wavelength of 375 nm was chosen as the optimal excitation light source to investigate the ALP sensing performance in the subsequent experiments. Other conditions that influenced the sensing performance such as the enzymatic incubation time, the concentration of OPD, MnO_2 nanosheets, and AAP were also optimized, respectively. As shown in Fig. S10 (ESI†), at a reaction time of 50 min, the optimal contents of 0.8 mM OPD, 5 μg mL^{-1} MnO_2 nanosheets, and 0.5 mM AAP were chosen for ALP sensing. To ensure the applicability of the proposed system in the practical bioanalysis, a temperature of 37 °C and the Tris-HCl buffer of pH 7.4 were used. The fluorescent photos and the fluorescence spectra of the proposed ratiometric sensing platform with varied ALP contents are obtained. As shown in Fig. 3A, with the increase of the ALP concentrations from 0 to 200 mU mL^{-1}, the color of the system photographed under 365 nm UV irradiation was gradually changed from yellow to yellowish and then to white and blue, indicating a sensitive colorimetric response of this fluorescent system toward ALP content. It is clear that the fluorescence intensity of DFQ at 430 nm gradually increased but that of oxOPD at 563 nm correspondingly decreased with increasing ALP from 0 to 200 mU mL^{-1} (Fig. 3B). It was found that the F_{563}/F_{430} was proportional to the concentration of ALP within a range of 0.25–10 mU mL^{-1} with the linear regression equation of $F = 21.25–2.092 \times C_{ALP}$ and the square of the correlation coefficient of 0.9983 (Fig. 3C). The calculated LOD was 0.06 mU mL^{-1} based on $3\sigma/k$ (k of 2.092 and σ of 0.0418 are the slope of the obtained regression equation and the standard deviation of blank signals of 20 measurements, respectively). To our knowledge, this ratio fluorometric bioassay has a satisfactory LOD compared to many reported methods (Table S1, ESI†), suggesting a good sensing performance of our developed method toward ALP detection. In addition, it is worth noting that this proposed ratio sensing platform has high selectivity toward ALP detection. As shown in Fig. 4, in the presence of typical potential substances such as HRP, Trypsin, AChE, Lysozyme, Cellulase, Gox, BSA, and Protease with a higher content (80 mU mL^{-1}), only target ALP (8 mU mL^{-1}) caused a significant decrease in the fluorescence intensity ratio (F_{563}/F_{430}) and no obvious readout change for the system without ALP addition. More significantly, we subsequently found that some reducing substances like cysteine and glutathione did not interfere with the

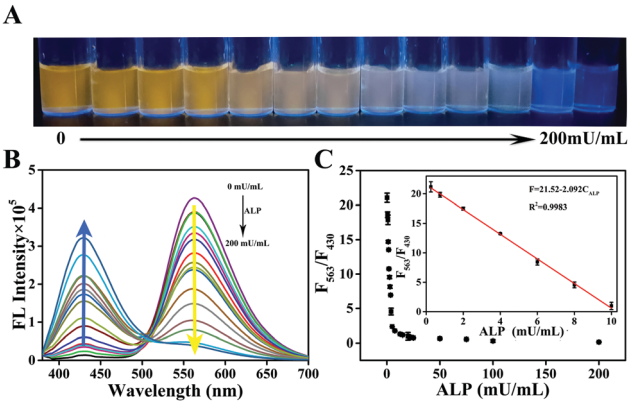

Fig. 3 (A) Photos of the corresponding sensing system under 365 nm ultraviolet light upon different ALP concentrations. (B) Fluorescence emission spectra of the sensing system in the presence of different concentrations of ALP. (C) Linear relationship between F_{563}/F_{430} and ALP concentration.

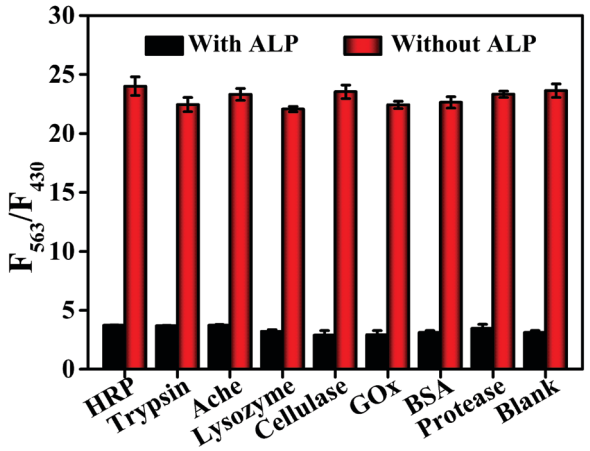

Fig. 4 The F_{563}/F_{430} of the proposed sensing system upon addition of ALP (8 mU mL^{-1}) and the control enzymes/proteins (80 mU mL^{-1}).

ALP determination of this proposed ratio fluorometric bioassay (Fig. S11, ESI†).

To further validate the potential applicability of this ratio fluorescence method, we tested ALP in practical serum samples by using the standard addition method. As displayed in Table S2 (ESI†), the recoveries range from 98.0% to 105.0% with a relative standard deviation (RSD) of 1.20–3.40%, indicating the potential accuracy and reliability of this ratio fluorometric bioassay for ALP activity analysis in real samples. It is worth noting that our developed ratio fluorometric system could be extended to sensitively screen inhibitors of ALP by using Na_3VO_4 as the inhibitor model. As depicted in Fig. S12 (ESI†), the IC_{50} value (concentrations of inhibitor when the ALP activity is inhibited by 50%) was calculated to be 24.21 μM, which is in good agreement with the previous report.[33]

In conclusion, we proposed a ratio fluorometric sensing platform to sense ALP activity based on the novel conversion from one fluorescent signal precursor to two fluorescent signal indicators using the superior oxidation capability of MnO_2 nanosheets. Due to the indirect mediation effect of target ALP to the generation of the intermediate AA and the fluorescent signal of DFQ as well as the decrease of the fluorescent signal of oxOPD, the developed ratio fluorometric system exhibited robust ratiometric fluorescence response to ALP activity with high selectivity and sensitivity. Since this ratio fluorometric strategy for ALP sensing exhibits good simplicity, low cost and popular operation, it will hold great potential in the biological sensing field and other analysis fields.

The authors gratefully acknowledge the financial support from the National Natural Science Foundation of China (22064014, 21765013), the Key Talent Project of Gansu Province (2019-115, 2019-39) and the Feitian Scholar Program of Gansu Province.

Conflicts of interest

There are no conflicts to declare.

Notes and references

1 K. Stefkova, J. Prochazkova and J. Pachernik, *Stem Cells Int.*, 2015, **11**, 628368.
2 K. Ooi, K. Shiraki, Y. Morishita and T. Nobori, *J. Clin. Lab. Anal.*, 2007, **21**, 133–139.
3 M. Kawaguchi, K. Hanaoka, T. Komatsu, T. Terai and T. Nagano, *Bioorg. Med. Chem. Lett.*, 2011, **21**, 5088–5091.
4 Y. Choi, N. H. Ho and C. H. Tung, *Angew. Chem., Int. Ed.*, 2007, **46**, 707–709.
5 Z. Gao, K. Deng, X. D. Wang, M. Miro and D. Tang, *ACS Appl. Mater. Interfaces*, 2014, **6**, 18243–18250.
6 T. Wu, Z. Ma, P. Li, M. Liu, X. Liu, H. Li, Y. Zhang and S. Yao, *Talanta*, 2019, **202**, 354–361.
7 S. Goggins, C. Naz, B. J. Marsh and C. G. Frost, *Chem. Commun.*, 2015, **51**, 561–564.
8 K. Ino, Y. Kanno, T. Arai, K. Y. Inoue, Y. Takahashi, H. Shiku and T. Matsue, *Anal. Chem.*, 2012, **84**, 7593–7598.
9 C. Chen, D. Zhao, B. Wang, P. Ni, Y. Jiang, C. Zhang, F. Yang, Y. Lu and J. Sun, *Anal. Chem.*, 2020, **92**, 4639–4646.
10 C. Chen, G. Zhang, P. Ni, Y. Jiang, Y. Lu and Z. Lu, *Microchim. Acta*, 2019, **186**, 348.
11 X. Wu, Y. Diao, C. Sun, J. Yang, Y. Wang and S. Sun, *Talanta*, 2003, **59**, 95–99.
12 A. Ingram, B. D. Moore and D. Graham, *Bioorg. Med. Chem. Lett.*, 2009, **19**, 1569–1571.
13 H. Liu, M. Li, Y. Xia and X. Ren, *ACS Appl. Mater. Interfaces*, 2017, **9**, 120–126.
14 Q. Li, C. Wang, H. Tan, G. Tang, J. Gao and C.-H. Chen, *RSC Adv.*, 2016, **6**, 17811–17817.
15 J. Liu, D. Tang, Z. Chen, X. Yan, Z. Zhong, L. Kang and J. Yao, *Biosens. Bioelectron.*, 2017, **94**, 271–277.
16 Z. Qian, L. Chai, C. Tang, Y. Huang, J. Chen and H. Feng, *Anal. Chem.*, 2015, **87**, 2966–2973.
17 K. Zhang, H. Zhou, Q. Mei, S. Wang, G. Guan, R. Liu, J. Zhang and Z. Zhang, *J. Am. Chem. Soc.*, 2011, **133**, 8424–8427.
18 D. Gong, S. C. Han, A. Iqbal, J. Qian, T. Cao, W. Liu, W. Liu, W. Qin and H. Guo, *Anal. Chem.*, 2017, **89**, 13112–13119.
19 M. Wang, S. Wang, X. Xie and X. Su, *ACS Appl. Nano Mater.*, 2020, **3**, 6034–6042.
20 P. K. Mehta, G. W. Hwang, J. Park and K.-H. Lee, *Anal. Chem.*, 2018, **90**, 11256–11264.
21 M. Cai, C. Ding, F. Wang, M. Ye, C. Zhang and Y. Xian, *Biosens. Bioelectron.*, 2019, **137**, 148–153.
22 X. L. Zhang, C. Zheng, S. S. Guo, J. Li, H. H. Yang and G. Chen, *Anal. Chem.*, 2014, **86**, 3426–3434.
23 T. Xiao, J. Sun, J. Zhao, S. Wang, G. Liu and X. Yang, *ACS Appl. Mater. Interfaces*, 2018, **10**, 6560–6569.
24 J. He, X. Jiang, P. Ling, J. Sun and F. Gao, *ACS Omega*, 2019, **4**, 8282–8289.
25 S. He, B. Song, D. Li, C. Zhu, W. Qi, Y. Wen, L. Wang, S. Song, H. Fang and C. Fan, *Adv. Funct. Mater.*, 2010, **20**, 453–459.
26 W. Zhai, C. Wang, P. Yu, Y. Wang and L. Mao, *Anal. Chem.*, 2014, **86**, 12206–12213.
27 G. Zhang, L. Ren, Z. Yan, L. Kang, Z. Lei, H. Xu, F. Shi and Z. H. Liu, *Chem. Commun.*, 2017, **53**, 2950–2953.
28 Y. Liu, M. Pan, W. Wang, Q. Jiang, F. Wang, D. Pang and X. Liu, *Anal. Chem.*, 2019, **91**, 2086–2092.
29 J. Yang, Q. Ma, F. Huang, L. Sun and J. Dong, *Anal. Lett.*, 1998, **31**, 2757–2766.
30 D. Zhao, J. Li, C. Peng, S. Zhu, J. Sun and X. Yang, *Anal. Chem.*, 2019, **91**, 2978–2984.
31 A. Kokado, H. Arakawa and M. Maeda, *Anal. Chim. Acta*, 2000, **407**, 119–125.
32 X. Li, L. Zhu, Y. Zhou, H. Yin and S. Ai, *Anal. Chem.*, 2017, **89**, 2369–2376.
33 J. Zhao, S. Wang, S. Lu, X. Bao, J. Sun and X. Yang, *Anal. Chem.*, 2018, **90**, 7754–7760.